

Classical Novae as a Probe of the Cataclysmic Variable Population

Dean M. Townsley – University of California

Lars Bildsten – University of California

Deposited 08/22/2018

Citation of published version:

Townsley, D., Bildsten, L. (2005): Classical Novae as a Probe of the Cataclysmic Variable Population. *The Astrophysical Journal*, 628(1). <http://dx.doi.org/10.1086/430594>

CLASSICAL NOVAE AS A PROBE OF THE CATAclySMIC VARIABLE POPULATION

DEAN M. TOWNSLEY¹

Department of Physics, Broida Hall, University of California, Santa Barbara, CA 93106

AND

LARS BILDSTEN

Kavli Institute for Theoretical Physics and Department of Physics, Kohn Hall, University of California,
Santa Barbara, CA 93106; bildsten@kitp.ucsb.edu

Received 2005 January 4; accepted 2005 March 22

ABSTRACT

Classical novae (CNe) are the brightest manifestation of mass transfer onto a white dwarf (WD) in a cataclysmic variable (CV). As such, they are probes of the mass transfer rate, \dot{M} , and WD mass, M_{WD} , in these interacting binaries. Our calculations of the dependence of the CN ignition mass, M_{ign} , on \dot{M} and M_{WD} yields the recurrence times of these explosions. We show that the observed CNe orbital period distribution is consistent with the interrupted magnetic braking evolutionary scenario, in which at orbital periods $P_{\text{orb}} > 3$ hr mass transfer is driven by angular momentum loss via a wind from the companion star, and at $P_{\text{orb}} < 3$ hr by gravitational radiation. About 50% of CNe occur in binaries accreting at $\dot{M} \simeq 10^{-9} M_{\odot} \text{ yr}^{-1}$ with $P_{\text{orb}} = 3\text{--}4$ hr, with the remaining 50% split evenly between P_{orb} longer (higher \dot{M}) and shorter (lower \dot{M}) than this. This resolution of the relative contribution to the CN rate from different CVs tells us that $3(9) \times 10^5$ CVs with WD mass $1.0(0.6) M_{\odot}$ are needed to produce one CN per year. In addition, one CN per year requires a CV birthrate of $1(2) \times 10^{-4} \text{ yr}^{-1}$ and likely ejects mass into the interstellar medium at a rate of $\dot{M} = 3(9) \times 10^{-5} M_{\odot} \text{ yr}^{-1}$. Using the *K*-band-specific CN rate measured in external galaxies, we find a CV birthrate of $2(4) \times 10^{-4} \text{ yr}^{-1}$ per $10^{10} L_{\odot, K}$, very similar to the luminosity specific Type Ia supernova rate in elliptical galaxies. Likewise, we predict that there should be 60–180 CVs for every $10^6 L_{\odot, K}$ in an old stellar population. The population of X-ray-identified CVs in the globular cluster 47 Tuc is similar to this number, showing no overabundance relative to the field. The observed CN P_{orb} distribution also contains evidence for a CV population that has no period gap. These are likely systems with a strongly magnetic WD (polars) in which it has been suggested that the field interferes with the wind of the companion, limiting angular momentum losses to those of gravitational radiation and eliminating the period gap. With this reduced \dot{M} , polars evolve more slowly than systems that undergo magnetic braking. Using a two-component steady state model of CV evolution, we show that the fraction of CVs that are magnetic (22%) implies a birthrate of 8% relative to nonmagnetic CVs, similar to the fraction of strongly magnetic field WDs.

Subject headings: binaries: close — novae, cataclysmic variables — stars: statistics — white dwarfs

1. INTRODUCTION

A classical nova (CN) outburst is the result of a thermonuclear runaway in the hydrogen-rich accreted layers on a white dwarf (WD) in a mass-transferring cataclysmic variable (CV) binary (see Shara 1989 for a review). The number of CNe with measured orbital periods, P_{orb} , has been increasing; Diaz & Bruch (1997) made a first comparison to the CN period distribution with 30 objects, and recently Warner (2002) listed P_{orb} for 50 CNe. These range from 1.4 to more than 16 hr, with most below 5 hr. CVs (Warner 1995) consist of a WD primary accreting mass from a normal low-mass star that is filling its Roche lobe and spend most of their life accreting at rates $\dot{M} \approx 10^{-9}$ – $10^{-11} M_{\odot} \text{ yr}^{-1}$ (e.g., Howell et al. 2001; hereafter HNR01). CVs are formed when the companion (of mass M_2) to a WD (made during a common-envelope event) comes into contact with its Roche lobe as a result of angular momentum losses. The CV evolves toward shorter orbital periods as the binary loses angular momentum at a rate \dot{J} , and the companion transfers mass to the WD at a rate \dot{M} . The orbital period distribution of CN, a direct

reflection of the CN frequency, provides a diagnostic of \dot{M} in CVs over the time to accumulate an unstable layer, 10^5 – 10^7 yr.

It is generally thought that the paucity of CVs with $2 \text{ hr} \lesssim P_{\text{orb}} \lesssim 3 \text{ hr}$ (e.g., Shafter 1992), the so-called period gap, is due to switching between a high \dot{J} state above 3 hr to a comparatively low \dot{J} state below 3 hr (e.g., HNR01). Upon such a sudden reduction in \dot{J} , the requisite reduction in \dot{M} causes the companion, which has been slightly out of thermal equilibrium due to the high mass-loss rate, to contract and fall inside the Roche lobe, halting mass transfer. Eventually, as P_{orb} continues to decrease due to angular momentum loss, Roche lobe contact is reestablished. The simplest paradigm of CV evolution holds that \dot{J} is determined by the WD mass M_{WD} , M_2 , and P_{orb} . Interrupted magnetic braking (IMB) has arisen as a good candidate for \dot{J} prescriptions (see, e.g., Paczynski & Sienkiewicz 1983; Rappaport et al. 1983; Spruit & Ritter 1983; Hameury et al. 1988; Kolb 1993; HNR01). In the IMB scenario, \dot{J} is initially driven by angular momentum lost in the stellar wind of the secondary star (Verbunt & Zwaan 1981) for $P_{\text{orb}} \gtrsim 3$ hr. The magnetic braking is interrupted (potentially by the loss of the radiative core), and \dot{J} falls to the rate set by gravitational radiation (see, e.g., Faulkner 1971; Paczynski & Sienkiewicz 1981; Rappaport et al. 1982). IMB explains the period gap of the CV population, and the predicted $\langle \dot{M} \rangle$ agrees with observations of the WD surface

¹ Current address: Department of Astronomy and Astrophysics, 5640 South Ellis Avenue, University of Chicago, Chicago, IL 60637; townsley@uchicago.edu.

temperatures (Townsend & Bildsten 2003). This agreement is somewhat surprising, because modern measurements of \dot{J} for isolated low-mass stars do not appear to follow the law used in the IMB scenario (Andronov et al. 2003). IMB also makes a very important but unconfirmed prediction: that CVs evolve across the period gap.

For a given composition of accreted material, there are three independent parameters that set M_{ign} , and thus the CN rate: \dot{M} , T_c , and M_{WD} . Many previous studies (e.g., Truran & Livio 1986; Ritter et al. 1991) focused only on the dependence of the CN frequency on M_{WD} . Here we focus on T_c 's dependence on \dot{M} . Townsend & Bildsten (2004; hereafter TB04) showed that, after extended accretion and many CN cycles, T_c is set by \dot{M} because of the accretion's impact on the thermal state of the WD core during the long interval between CNe. Given any $\dot{M}(P_{\text{orb}})$ relation, TB04's calculation of T_c enables the first consistent prediction of how the CN rate varies with orbital period. Using \dot{M} -dependent M_{ign} values calculated at several T_c values (Priyalnik & Kovetz 1995), Nelson et al. (2004) showed clearly that this knowledge of T_c is essential for a conclusive prediction of the P_{orb} distribution. In § 2 we briefly review the work of TB04, and in § 3 we apply it to calculate the CN period distribution and compare it to that observed. We find that IMB is remarkably consistent with the observed CN frequency, yielding a firm relationship between observed CN frequency and the CV population. Confirming this scenario finally allows us to use the observed CN rate to infer the number of underlying CVs. This impacts searches for CVs in the field, as well as in globular clusters, as we note in § 4.

2. CLASSICAL NOVA IGNITION MASSES

IMB predicts that typical accretion rates near $P_{\text{orb}} = 3\text{--}4$ hr are $\dot{M} \simeq 10^{-9} M_{\odot} \text{ yr}^{-1}$ and decrease to $\dot{M} \simeq 5 \times 10^{-11} M_{\odot} \text{ yr}^{-1}$ below 2 hr. This factor of 20 drop in \dot{M} across the period gap requires that the \dot{M} dependence of M_{ign} be taken into account when explaining the orbital period distribution of CN. These two \dot{M} s lead to different ignition modes. For the higher \dot{M} , TB04 found that the CN is triggered by trace ${}^3\text{He}$ in the accreted material (Shara 1980), leading to a CNO-burning runaway in a radiative layer. At the lower \dot{M} , however, the CN outburst is triggered by the p - p chain when the base of the accreted shell is conductive. This wide range of conditions means that the prior prescriptions of ignition, such as a single, unique pressure (Gehrz et al. 1998; Warner 2002) or taking M_{ign} independent of \dot{M} (Ritter et al. 1991; Diaz & Bruch 1997), are wholly inadequate.

By considering the release of energy due to compression of the accreted layers, TB04 calculated the rate of heat loss or gain of the WD core. This rate varies as the accreted layer builds up, and by taking the average loss or gain to be zero, TB04 found an equilibrium, $T_{c,\text{eq}}$, which the WD will approach under prolonged accretion. For $P_{\text{orb}} \gtrsim 3$ hr, the magnetic braking phase, the WD has only marginally enough time, $\sim 10^7$ yr, to reach $T_{c,\text{eq}}$. However, at these accretion rates, M_{ign} is insensitive to T_c if it is lower than $T_{c,\text{eq}}$, because the ignition occurs in a layer that is not conductively coupled to the core. Hence, the temperature is set by the response of the envelope to the energy being released by compression (TB04). At lower \dot{M} , T_c determines M_{ign} , but the low \dot{M} state for CVs is long-lived ($> 10^9$ yr), allowing the WD core to reach $T_{c,\text{eq}}$. Thus, for CV evolution, use of $T_{c,\text{eq}}$ provides M_{ign} values that are self-consistent and independent of assumptions about the WD thermal state. This is in contrast to all prior M_{ign} calculations (see, e.g., Fujimoto 1982; MacDonald 1984; Priyalnik & Kovetz 1995). The T_c values found by TB04 are $\leq 10^7$ K

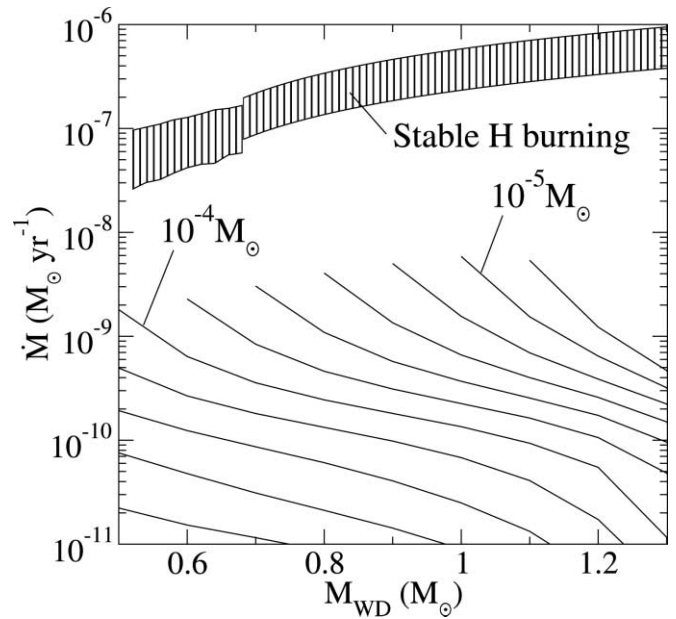


FIG. 1.— Classical nova ignition masses, M_{ign} , for WDs that have reached their equilibrium core temperature, as determined by TB04. Contours are evenly spaced in $\log(M_{\text{ign}})$; labels indicate M_{ign} in M_{\odot} . The vertically hatched region indicates where steady burning of H is expected (Piersanti et al. 2000; Nomoto 1982). At higher \dot{M} , envelope buildup and expansion into a giant is expected.

for $M_{\text{WD}} < 1.2 M_{\odot}$, lower than the lowest T_c considered by Priyalnik & Kovetz (1995) in their broad parameter survey.

Models of donor evolution in CVs (D'Antona & Mazzitelli 1982; Iben & Tutukov 1984; McDermott & Taam 1989) show that the ${}^3\text{He}$ abundance reaches mass fractions of $X_{{}^3\text{He}} \simeq 0.001$ when the orbital period is 3–4 hr (the companion mass is below $\simeq 0.4 M_{\odot}$). This is when the star has lost enough mass and the convection layer has become deep enough that the partially fused material in the stellar interior is uncovered. Precisely when this occurs, and the $X_{{}^3\text{He}}$ reached, is sensitive to the donor's initial mass, but generally does not exceed 0.003. We are most interested in CN rates for $P_{\text{orb}} \leq 4$ hr, so we include a fraction $X_{{}^3\text{He}} = 0.001$ in our ignition models.

The M_{ign} results of TB04 are shown in Figure 1. Compared to previous ignition mass calculations, TB04 found larger M_{ign} at $\dot{M} \lesssim 10^{-10} M_{\odot} \text{ yr}^{-1}$, due to the lower T_c , and similar M_{ign} at $\dot{M}_{\text{ign}} \gtrsim 10^{-9} M_{\odot} \text{ yr}^{-1}$, due to offsetting effects of the lower T_c and the inclusion of ${}^3\text{He}$ leading to an earlier trigger. TB04 found that for the few systems that have a known ejected mass and P_{orb} (giving some indication of \dot{M}), the ejected masses are similar to M_{ign} , implying that each CN ejects approximately the amount of material accreted since the last event. TB04's results do not show the trivial $M_{\text{ign}} \propto R^4/M_{\text{WD}}$ scaling assumed for a unique ignition pressure (see their discussion). An ignition pressure of $p = 2 \times 10^{19}$ dyne cm^{-2} would have 10^{-5} , 10^{-4} , and $10^{-3} M_{\odot}$ contours, which are vertical lines at $M_{\text{WD}} = 1.3$, 1.0, and $0.58 M_{\odot}$. (This ignition pressure is used by Gehrz et al. [1998] in their discussion of the nucleosynthetic impact of nova ejecta.) As we will see, most CNe have $\dot{M} \sim 10^{-9} M_{\odot} \text{ yr}^{-1}$, and thus lower M_{ign} than this prescription implies.

Also shown in Figure 1 is the region (vertically hatched) where steady burning is expected. For $0.52 \leq M_{\text{WD}}/M_{\odot} \leq 0.68$, the calculations of Piersanti et al. (2000) are shown. For $M_{\text{WD}} \geq 0.6 M_{\odot}$, the upper bound is found from the core mass-luminosity relation of Paczyński (1970), and the lower bound is taken to be 0.4 of this

(Nomoto 1982). At higher \dot{M} , envelope buildup and expansion into a giant is expected.

3. THE CLASSICAL NOVAE ORBITAL PERIOD DISTRIBUTION

The observed distribution of CN orbital periods (Warner 2002) is shown in Figure 2 by the thin solid line. These data differ only very slightly from the collection in Ritter & Kolb (2003).² We have neglected any selection effects, as they have not been satisfactorily quantified to date. These are complex, so we will not attempt a conclusive discussion, but only mention two important ones, CN outburst brightness and remnant brightness. The tables in Prialnik & Kovetz (1995), for the coldest T_c and $M_{WD} = 1 M_\odot$, imply that CN outbursts for systems with $\dot{M} \sim 10^{-10} M_\odot \text{ yr}^{-1}$ are 3–4 times as bright as those for systems with $\dot{M} \sim 10^{-8} M_\odot \text{ yr}^{-1}$. However, the spatial distribution in the Galaxy and the effects of absorption must be considered in order to judge how the observed population reflects this brightness variation (see Ritter et al. 1991 for some discussion). It is likely that remnant brightness depends on \dot{M} , and thus P_{orb} , introducing additional selection effects in remnant recovery and characterization.

3.1. Using Previous Population Synthesis Calculations

In order to calculate the CN frequency, we must first use the IMB prescriptions to obtain \dot{M} from P_{orb} . Since the secondary fills its Roche lobe, P_{orb} is directly related to M_2 by its mass-radius relation. We enforce $R_2 = 0.46a[M_2/(M_{WD} + M_2)]^{1/3}$, so that $P_{orb} = 9 \text{ hr} (M_2/M_\odot)^{-1/2} (R_2/R_\odot)^{3/2}$. To reproduce IMB for $P_{orb} > 3 \text{ hr}$, we use the magnetic braking law from HNR01 (see also Rappaport et al. 1983)

$$\dot{J}_{MB} = -9.4 \times 10^{38} \text{ ergs} \left(\frac{M_2}{M_\odot} \right) \left(\frac{R_2}{R_\odot} \right)^3 \left(\frac{P_{orb}}{\text{hr}} \right)^{-3}. \quad (1)$$

When the binary is evolving under the influence of magnetic braking, the \dot{M}_2 is large enough that the secondary is out of thermal equilibrium and therefore has a larger radius than a main-sequence star of the same mass (the effect that leads to the period gap). In order to account for this, we use the M_2 - R_2 relation found by HNR01 using a bipolytrope model for the secondary and evolving under equation (1), $R_2/R_\odot = 0.81(M_2/M_\odot)^{0.67}$. For $P_{orb} < 3 \text{ hr}$, we apply gravitational radiation losses given by

$$\begin{aligned} \dot{J}_{gr} &= -\frac{32GQ^2\omega^5}{5c^5} \\ &= -2.7 \times 10^{37} \text{ ergs} \left(\frac{a}{R_\odot} \right)^4 \left(\frac{M_{WD}M_2}{M_t M_\odot} \right)^2 \left(\frac{P_{orb}}{\text{hr}} \right)^{-5}, \end{aligned} \quad (2)$$

where Q is the moment of the binary about the orbital center, $\omega = 2\pi/P_{orb}$, a is the orbital separation, and $M_t = M_{WD} + M_2$. We use $R_2/R_\odot = 0.71(M_2/M_\odot)^{0.77}$ for a star in thermal equilibrium, also from HNR01. These M_2 - R_2 relations give a period gap (transition from the former to the latter) at 2–3 hr when the donor is $0.21 M_\odot$, as found for this “standard model” (Model A) in HNR01.

In addition to M_{ign} and the IMB prescriptions, we also require a CV population model to construct the CN orbital period distribution. Detailed Monte Carlo CV population models are explored by HNR01 and by Nelson et al. (2004), in the same context as here, but without the TB04 predictions of T_c from \dot{M} .

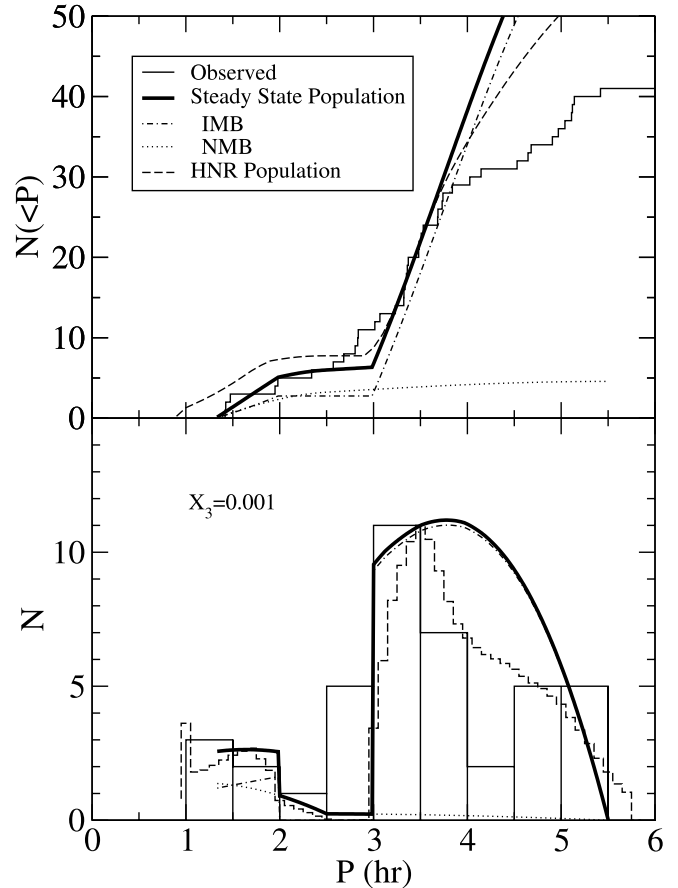


FIG. 2.—Cumulative (top panel) and normal (bottom panel) distribution of classical novae orbital periods. The thin solid lines show the observed distribution, with the nine systems with $P_{orb} > 6 \text{ hr}$ not shown. The steady state population described in the text (thick solid line) consists of an equal number of CVs that undergo an interrupted magnetic braking episode (IMB population; dot-dashed line) and that undergo no magnetic braking (NMB population; dotted line). This combined population reproduces the major features of the cumulative distribution for $P_{orb} \lesssim 4 \text{ hr}$. A full population synthesis (HNR01; dashed line) including only objects that undergo a magnetic braking phase displays similar features, matching the observed distribution remarkably well. A mass fraction $X_{3\text{He}} = 0.001$ is used for all.

HNR01 calculated the number of CVs per period interval, which we denote n_p so that $n_p dP$ is the number with orbital periods between P and $P + dP$. We use a single characteristic mass in lieu of a detailed M_{WD} distribution. For the HNR01 population we use $M_{WD} = 0.72 M_\odot$, the average CN M_{WD} for their populations, and $X_{3\text{He}} = 0.001$.

Using the above relationships to obtain \dot{M} , n_p from HNR01, and the M_{ign} from TB04, the resulting CN distribution is shown by the dashed line in Figure 2 and is normalized to match at $P_{orb} = 3.5 \text{ hr}$. The most noticeable difference between this and our steady state model presented below (thick solid line) is how the CV population based on HNR01 drops off at long P_{orb} due to the CVs being born throughout the 3.5–6 hr range. The exact form of this turnover depends on the common-envelope phase (Nelson et al. 2004) through the orbital period distribution of the common-envelope products. By construction, the HNR01 distribution lacks systems in the period gap. Every system that comes into contact with a companion that has a radiative core ($P_{orb} \gtrsim 2.4 \text{ hr}$) goes through a MB phase. This distribution matches quite well in both the 1–2 and 3–4 hr regions, keeping in mind the \sqrt{N} noise present in the observed distribution. The HNR01 population extends down to 1 hr due to the famous discrepancy in the

² See also updates available at <http://physics.open.ac.uk/RKcat/>.

period minimum between observation and theory (Kolb & Baraffe 1999).

3.2. Simpler Population Calculations

In order to understand how the P_{orb} distribution depends separately on the distribution of \dot{M} and the CV birth distribution, we also construct a steady state population with a specified birth distribution. CVs are born (i.e., come into contact and initiate mass transfer for the first time) at a variety of orbital periods determined by the distribution of M_{WD} and M_2 after the common-envelope event. For a population of n_P CVs per period interval with characteristic mass M_{WD} , conservation implies

$$\frac{\partial n_P}{\partial t} = \frac{\partial(n_P \dot{P}_{\text{orb}})}{\partial P_{\text{orb}}} + b_P, \quad (3)$$

where b_P is the CV birthrate per period interval, i.e., the number of CVs per year that commence accretion for the first time between P and $P + dP$. We assume that all matter accreted from the companion is ejected in the CN, consistent with current observations (TB04), so that M_{WD} is constant. We also assume that the CV birthrate has been constant over the last 4 Gyr, the time it takes a CV to reach the period minimum at $P_{\text{orb}} \simeq 80$ minutes (HNR01). Beyond this point the companion becomes essentially fixed in radius, so that the binary expands and \dot{M} drops quickly. These assumptions give a steady state ($\partial n_P / \partial t = 0$) CV population whose number density per period interval from equation (3) is

$$n_P = \frac{1}{|\dot{P}_{\text{orb}}|} \int_{\infty}^{P_{\text{orb}}} b_P dP, \quad (4)$$

where we assume no systems at large P_{orb} .

As noted above, the secondary's mass-radius relation is well characterized by a power law, and so for Roche Lobe filling systems $\alpha \equiv d \ln P_{\text{orb}} / d \ln M_2$ is approximately a constant, typically between 0.5 and 1. Thus $\dot{P}_{\text{orb}} = -\dot{M} \alpha P_{\text{orb}} / M_2$ and the CN frequency per period interval is

$$\nu_P \equiv \frac{\dot{M}}{M_{\text{ign}}} n_P \propto \frac{M_2 / P_{\text{orb}}}{M_{\text{ign}}}. \quad (5)$$

The direct dependence on \dot{M} cancels for this observable. By far the most important part of the remaining \dot{M} dependence is in M_{ign} . Evaluating across the period gap, M_2 is constant, while P_{orb} changes by 50% due to bloating of the companion above the gap. On the other hand \dot{M} is expected to change from 10^{-9} to $\simeq 5 \times 10^{-11} M_{\odot} \text{ yr}^{-1}$, causing M_{ign} (from Fig. 1) to increase from $\simeq 10^{-5}$ to $\gtrsim 10^{-4} M_{\odot}$, a factor of >10 . Thus the CN orbital period distribution directly reflects \dot{M} through its effect on M_{ign} . With the consistent calculation of M_{ign} from \dot{M} provided by TB04, we can probe the \dot{M} - P_{orb} relation directly by comparing the steady state population to observations. Evidence for evolution across the gap is then contained in the degree to which a single steady state distribution can reproduce the observations.

We use a binary with $M_{\text{WD}} = 1.0 M_{\odot}$ as representative, since the actual mass distribution is very sensitive to the common-envelope (CE) prescription (Nelson et al. 2004). Also, we set $X_{\text{He}} = 0.001$, because this is the approximate level expected in the accreted matter (see § 2). In order to account for the possibility of systems that do not undergo magnetic braking, we use three populations. The first follows the IMB scenario (the IMB

population), while the others only have J_{gr} applied (the NMB [no magnetic braking] populations). In the NMB case the secondary mass-radius relation is that of an equilibrium main-sequence star from HNR01.

Although the detailed form of the birth distribution above the gap is sensitive to the CE prescription (HNR01; Nelson et al. 2004), we employ a constant b_P between 3 and 5.5 hr for the IMB population. This captures the contrast in CN rate across the gap without depending explicitly on a particular CE prescription. CVs born with $P_{\text{orb}} \lesssim 2.5$ hr do not undergo magnetic braking in the IMB scenario. We call this population the NMBb (NMB below gap) population, and it has b_P constant between 1.3 and 2.5 hr. A second NMBa (NMB all periods) population represents systems that do not undergo magnetic braking regardless of their birth P_{orb} (see discussion of magnetic systems below). This population has a constant birth function between 1.3 and 5.5 hr. Note that, unlike the HNR01 population, we directly specify the minimum P_{orb} . These birthrates can then be used in equations (4) and (5), and the relative birth fractions for each population are given by $b_P(P_{\text{max}} - P_{\text{min}})$.

This steady state population is shown as the thick solid line in Figure 2, arbitrarily normalized to match the observed distribution (*thin solid line*) at 3.5 hr. The relative birth fractions for the curve shown are NMBa 8%, IMB 46%, and NMBb 46%. This model reproduces the major features of the observed population below 4 hr, including the slope in the cumulative distribution between 3 and 4 hr. The dependence on the common-envelope prescription and binary population parameters is essentially contained in the average M_{WD} , to which the shape of the curve is insensitive. The effect of a 30% change in M_{WD} is small compared to the >20 times difference in \dot{M} across the period gap.

The contrast in CN rate across the period gap does have some dependence on X_{He} . Under gravitational braking only, as is the case below the period gap, \dot{M} is low enough that M_{ign} is insensitive to X_{He} . However, the CN rate above the period gap, at which magnetic braking enhances \dot{M} , does depend on X_{He} . The dependence can be estimated by using the ignition density, $\rho_{\text{ign}} \propto T^{-3.2} X_{\text{He}}^{-1/2}$ from TB04, and combining it with an ideal gas equation of state, $M_{\text{ign}} \propto P_{\text{ign}} \propto \rho_{\text{ign}} T_{\text{ign}}$, and the power-law form of a free-free radiative envelope $T \propto P^{2/8.5}$, to obtain $\nu_P \propto 1/M_{\text{ign}} \propto X_{\text{He}}^{0.33}$. This scaling is confirmed by numerical calculations. Thus, the expected maximum value of $X_{\text{He}} = 0.003$ (see § 2) leads to a 50% enhancement of the CN rate above the period gap over $X_{\text{He}} = 0.001$. Matching this new normal distribution to the observations at 3.5 hr, the rate below the gap is $\frac{2}{3}$ of that shown in Figure 2, still consistent with the observations. Thus the value we have adopted, $X_{\text{He}} = 0.001$ is expected from donor evolution and provides the best fit to the data when birthrates above and below the period gap are assumed to be approximately equal.

The observed orbital period distribution of CN is consistent with CVs evolving across the period gap and magnetic braking between 3 and 4 hr governed by a law like equation (1). As shown by the thick (model) and thin (data) solid lines in Figure 2, the contrast between the 1–2 and the 3–4 hr ranges is of the appropriate size for a population in which \dot{J} above 3 hr is enhanced by magnetic braking. This contrast in CN rate is entirely due to the dependence of M_{ign} on \dot{M} .

3.3. Magnetic Accretors with No Magnetic Braking

The two components included in the model population, IMB and NMB, are also shown separately as the dot-dashed and dotted lines, respectively. These demonstrate the significant enhancement that magnetic braking implies in the CN rate over gravitational

radiation alone. The prediction of a NMB model with $b_p = 0$ (all systems being born at long periods) falls weakly to shorter orbital period in the normal distribution, as for the IMB curve below 2 hr. With a constant b_p , a NMB model monotonically increases to shorter orbital periods, as seen for the dotted lines. Thus a NMB model alone is inconsistent with the observed orbital period distribution. The period distribution is also satisfactorily reproduced without the addition of the NMB population, making our confirmation of the IMB prescriptions and evolution across the gap robust with some evidence for additional systems in and below the gap. Measurement of this additional contribution is limited by the current quality of data.

There are two reasons a CV might not undergo the MB phase. For example, if MB cannot work when the companion is fully convective, then there is a minimum companion mass ($0.25 M_\odot$) for having an MB phase. We have implemented this by placing all systems born with $P_{\text{orb}} < 2.5$ hr in a NMB population. This can also be seen in the small number of systems between 2 and 2.5 hr in the HNR01 population. Additionally, motivated by the lack of a clear period gap for magnetic CVs (Verbunt 1997), Li et al. (1994) have conjectured that in polars the WD magnetic field prevents MB. Recent T_{eff} measurements of magnetic WDs (Araujo-Betancor et al. 2005; B. T. Gänsicke & D. M. Townsley 2005, in preparation) show that above the period gap, magnetic CVs have a significantly lower \dot{M} than dwarf novae at the same orbital period, providing direct evidence that magnetic CV evolution is quite different from that of nonmagnetic systems.

The absolute relative populations of magnetic and nonmagnetic CVs is not well known, because they are dominated by different and difficult-to-quantify selection effects. Approximately 22% of known CVs are magnetic (Araujo-Betancor et al. 2005). Using this steady state two-component population model, we find that, due to the slower evolution in the absence of MB, this requires that 8% of CVs born have strongly magnetic WDs, comparable to the fraction among field WDs (Jordan 1997; Wickramasinghe & Ferrario 2000). While giving tantalizing hints, the small number of observed systems makes it impossible to separate the prospective magnetic and nonmagnetic contributions to the NMB population.

4. DISCUSSION AND CONCLUSION

We have shown that a very simple CV population model with the assumptions of IMB and the M_{ign} calculated by TB04 reproduces the orbital period distribution of CNe, supporting the idea that CVs evolve across the period gap. This agreement is independent of the outcome of the common-envelope phase or properties of the primordial binary population. CNe are one CV phenomenon that is sensitive to \dot{M} averaged over the longest timescales, the CNe recurrence time, of 10^5 – 10^7 yr. The agreement with IMB provides additional evidence that the IMB prescriptions do indeed provide accurate long-term average \dot{M} for CVs. Townsley & Bildsten (2003) similarly found that the WD T_{eff} in dwarf nova systems, which reflects \dot{M} due to compression of the envelope, matches the predictions of IMB. The existence of CN with P_{orb} in the period gap implies that not all systems undergo IMB evolution, possibly due to inhibition of the secondary's wind by a strong WD magnetic field (Li et al. 1994). This inhibition will lead to slower evolution of magnetic CVs and thus increase their relative number in the CV population. We find that in order to obtain the 22% fraction of magnetic CVs observed (Araujo-Betancor et al. 2005), a relative birth fraction of magnetic CVs of 8% is required, comparable to the fraction among field WDs (Jordan 1997; Wickramasinghe & Ferrario 2000).

With a satisfactory \dot{M} distribution in hand, the total number of CNe observed provides a measurement of the CV population. This conversion does not depend directly on CE parameters, because a relatively small number of both observed novae and CVs in general have $P_{\text{orb}} > 4$ hr, for which the birth distribution is important. The conversion does, however, depend on the typical WD mass, due to its importance in setting M_{ign} . Note also that while most CV WDs have $M_{\text{WD}} \lesssim 0.7 M_\odot$, including many helium WDs (HNR01), the average CN mass is sensitive to the upper end of the mass distribution (Nelson et al. 2004). Knowledge of the \dot{M} distribution allows proper adjustment for the fact that while most CVs are below the period gap, most CNe are in CVs above the period gap. This is a fairly short-lived period of the CV's lifetime, lasting only ~ 100 Myr (HNR01), which is preceded by the post-common-envelope in-spiral and followed by accretion below the period gap during which the CN rate is much lower. We find that one CN per year implies 3×10^5 (9×10^5) CVs above the period minimum, $t \lesssim 3$ Gyr (4 Gyr), and a CV birthrate of 10^{-4} yr^{-1} ($2 \times 10^{-4} \text{ yr}^{-1}$) if the average CN mass is $1.0 M_\odot$ ($0.6 M_\odot$).

Since pre-CVs finish the common-envelope phase with a wide range of orbital periods, the total CV and pre-CV population, and thus the CN rate, should relate to the total amount of low-mass stars, which is well represented by the K -band light. The apparent dependence of nova rate on stellar population is still uncertain, but points to these older populations. Surveys of nova rates in external galaxies (Williams & Shafter 2004) continue to show that the K -band-specific nova rate is about $2 \pm 1 \times 10^{-10} L_{\odot,K}^{-1} \text{ yr}^{-1}$ and does not depend strongly on galaxy type in nearby galaxies, with the exception of the LMC and SMC. M31 shows evidence that the CN rates might be dominated by the bulge population (Shafter & Irby 2001). Our work allows us to convert the K -band-specific nova rate into the CV population and birthrate, giving 60–180 CVs above the period minimum for every $10^6 L_{\odot,K}$ in an old stellar population and $2(4) \times 10^{-4}$ CVs born per year per $10^{10} L_{\odot,K}$. The 24–133 CVs estimated from *Chandra* observations of 47 Tuc (Heinke et al. 2005) is consistent with the 60–180 predicted by our work for the cluster mass ($10^6 M_\odot$; Pryor & Meylan 1993) and agrees with the CN rate implied by the one or two CNe observed in the last ~ 140 yr in the Galactic globular clusters (GCs) (Shara et al. 2004). Thus the GC CV population appears comparable to that in the field. The Type Ia supernova rate in elliptical galaxies is $3.5_{-1.1}^{+1.3} \times 10^{-4} \text{ yr}^{-1}$ per $10^{10} L_{\odot,K}$ (Mannucci et al. 2005), remarkably close to the CV birthrate. However, all indications are that the WD masses in CVs are not nearly large enough (TB03) to be Type Ia progenitors (Branch et al. 1995).

The local Galactic K -band luminosity density is 0.1 – $0.2 L_{\odot,K} \text{ pc}^{-3}$ (Olling & Merrifield 2001), giving a local CV space density of approximately $9(27) \times 10^{-6} \text{ pc}^{-3}$ again for an average mass of $1.0(0.6) M_\odot$. This agrees well with the $2 \times 10^{-5} \text{ pc}^{-3}$ found by Politano (1996) from a theoretical calculation of the CV birthrate. This space density is only slightly higher than the $6 \times 10^{-6} \text{ pc}^{-3}$ inferred from the PG survey (Ringwald 1996) but more than 10 times the $8 \times 10^{-7} \text{ pc}^{-3}$ obtained by Downes (1986). Both these survey numbers assume a scale height of CVs of 150 pc, whereas the above K -band luminosity density assumes a scale height of low-mass stars of 300 pc. Although more modern color-selected surveys exist, the lack of a broadly applicable, accurate CV distance measure hinders improved measurements of the space density.

In a similar manner, the total rate of matter injected into the interstellar medium (ISM) can be evaluated in terms of the CN outburst rate. Since we are assuming that all of the matter

transferred onto the WD is ejected in each CN outburst, this is just the average \dot{M} for the population times the total number of systems. We find that $3 \times 10^{-5} M_{\odot} \text{ yr}^{-1}$ ($9 \times 10^{-5} M_{\odot} \text{ yr}^{-1}$) is ejected into the ISM for each CN per year if the average CN mass is $1.0 M_{\odot}$ ($0.6 M_{\odot}$). The average initial mass of the donor contributes additional uncertainty but generally less than that due to the unknown average WD mass. Although somewhat lower than the value of $2 \times 10^{-4} M_{\odot}$ per CN outburst found by Truran & Livio (1986), these values are similar to the $\sim 10^{-4} M_{\odot}$ per outburst used by Gehrz et al. (1998) to estimate the impact of nucleosynthesis in CN outbursts on both the ISM and primordial solar system material. An interesting effect of the contrast in \dot{M} across the gap is that while approximately 85% of CN outbursts occur above the period gap and only 2% of pre-period-minimum systems are above the gap, approximately equal amounts of processed matter are contributed by objects above and below the period gap before the period minimum. This means that the type of CNe that are observed most often are only half the story for ISM injection.

With proper calibration, classical novae provide a useful standard candle for extragalactic distance measurements (della Valle & Livio 1995). The principle impediment to this usage is that the single measured parameter available for calibration, the

rate of decline, depends on M_{WD} , \dot{M} , and T_c . TB04 calculated T_c consistently from \dot{M} , eliminating it as a free parameter. Here we have demonstrated that IMB provides a satisfactory prediction of the \dot{M} distribution in the Galactic CV population, finding that CN outbursts occur predominantly when $\dot{M} \sim 10^{-9} M_{\odot} \text{ yr}^{-1}$, with a significant tail at lower \dot{M} . This leaves only M_{WD} to be calibrated from the rate of decline. Thus, with the support of theory, a statistically complete measurement of nova magnitudes and decline rates may be sufficient to measure the distance to an external galaxy.

We thank Boris Gänsicke for discussion and early access to observational data. This work was supported by the National Science Foundation under grants PHY 99-07949 and AST 02-05956 and by NASA through grant AR-09517.01-A from the Space Telescope Science Institute (STScI), which is operated by AURA, Inc., under NASA contract NAS5-26555. D. M. T. is supported by the NSF Physics Frontier Centers Joint Institute for Nuclear Astrophysics under grant PHY 02-16783, and D. O. E., under grant DE-FG 02-91ER 40606.

REFERENCES

- Andronov, N., Pinsonneault, M., & Sills, A. 2003, *ApJ*, 582, 358
 Araujo-Betancor, S., Gänsicke, B. T., Long, S. K., Beuermann, K., Sion, E. M., de Martino, D., & Szkody, P. 2005, *ApJ*, 622, 589
 Branch, D., Livio, M., Yungelson, L. R., Boffi, F. R., & Baron, E. 1995, *PASP*, 107, 1019
 D'Antona, F., & Mazzitelli, I. 1982, *ApJ*, 260, 722
 della Valle, M., & Livio, M. 1995, *ApJ*, 452, 704
 Diaz, M. P., & Bruch, A. 1997, *A&A*, 322, 807
 Downes, R. A. 1986, *ApJ*, 307, 170
 Faulkner, J. 1971, *ApJ*, 170, L99
 Fujimoto, M. Y. 1982, *ApJ*, 257, 767
 Gehrz, R. D., Truran, J. W., Williams, R. E., & Starrfield, S. 1998, *PASP*, 110, 3
 Hameury, J. M., King, A. R., Lasota, J. P., & Ritter, H. 1988, *MNRAS*, 231, 535
 Heinke, C. O., et al. 2005, *ApJ*, 625, 796
 Howell, S. B., Nelson, L. A., & Rappaport, S. 2001, *ApJ*, 550, 897 (HNR01)
 Iben, I., & Tutukov, A. V. 1984, *ApJ*, 284, 719
 Jordan, S. 1997, in *White Dwarfs: Proceedings of the 10th European Workshop on White Dwarfs*, ed. J. Isern, M. Hernanz, & E. García-Berro (Dordrecht: Kluwer), 397
 Kolb, U. 1993, *A&A*, 271, 149
 Kolb, U., & Baraffe, I. 1999, *MNRAS*, 309, 1034
 Li, J. K., Wu, K. W., & Wickramasinghe, D. T. 1994, *MNRAS*, 268, 61
 MacDonald, J. 1984, *ApJ*, 283, 241
 Mannucci, F., et al. 2005, *A&A*, 433, 807
 McDermott, P. N., & Taam, R. E. 1989, *ApJ*, 342, 1019
 Nelson, L. A., MacCannell, K. A., & Dubeau, E. 2004, *ApJ*, 602, 938
 Nomoto, K. 1982, *ApJ*, 253, 798
 Olling, R. P., & Merrifield, M. R. 2001, *MNRAS*, 326, 164
 Paczyński, B. 1970, *Acta Astron.*, 20, 47
 Paczyński, B., & Sienkiewicz, R. 1981, *ApJ*, 248, L27
 Paczyński, B., & Sienkiewicz, R. 1983, *ApJ*, 268, 825
 Piersanti, L., Cassisi, S., Iben, I. J., & Tornambé, A. 2000, *ApJ*, 535, 932
 Politano, M. 1996, *ApJ*, 465, 338
 Prialnik, D., & Kovetz, A. 1995, *ApJ*, 445, 789
 Pryor, C., & Meylan, G. 1993, in *ASP Conf. Ser. 50, Structure and Dynamics of Globular Clusters*, ed. S. G. Djorgovski & G. Meylan (San Francisco: ASP), 357
 Rappaport, S., Joss, P. C., & Webbink, R. F. 1982, *ApJ*, 254, 616
 Rappaport, S., Verbunt, F., & Joss, P. C. 1983, *ApJ*, 275, 713
 Ringwald, F. A. 1996, in *IAU Colloq. 158, Cataclysmic Variables and Related Objects*, ed. A. Evans & J. H. Wood (Dordrecht: Kluwer), 89
 Ritter, H., & Kolb, U. 2003, *A&A*, 404, 301
 Ritter, H., Politano, M., Livio, M., & Webbink, R. F. 1991, *ApJ*, 376, 177
 Shafter, A. W. 1992, *ApJ*, 394, 268
 Shafter, A. W., & Irby, B. K. 2001, *ApJ*, 563, 749
 Shara, M. M. 1980, *ApJ*, 239, 581
 ———. 1989, *PASP*, 101, 5
 Shara, M. M., Zurek, D. R., Baltz, E. A., Lauer, T. R., & Silk, J. 2004, *ApJ*, 605, L117
 Spruit, H. C., & Ritter, H. 1983, *A&A*, 124, 267
 Townsley, D. M., & Bildsten, L. 2003, *ApJ*, 596, L227
 ———. 2004, *ApJ*, 600, 390 (TB04)
 Truran, J. W., & Livio, M. 1986, *ApJ*, 308, 721
 Verbunt, F. 1997, *MNRAS*, 290, L55
 Verbunt, F., & Zwaan, C. 1981, *A&A*, 100, L7
 Warner, B. 1995, *Cataclysmic Variable Stars* (Cambridge: Cambridge Univ. Press)
 ———. 2002, in *AIP Conf. Proc. 637, Classical Nova Explosions*, ed. M. Hernanz & J. José (New York: AIP), 3
 Wickramasinghe, D. T., & Ferrario, L. 2000, *PASP*, 112, 873
 Williams, S. J., & Shafter, A. W. 2004, *ApJ*, 612, 867